Mongolian Journal of Chemistry
www.mongoliajol.info/index.php/MJC

Study of Oxadiazole derivatives as precursor for multi-functional inhibitor to SARS-CoV-2: A detailed virtual screening analysis

Vikash Kumar and Sumit Kumar*

Department of Chemistry, Magadh University, Bodh Gaya 824234, Bihar, India

* *Corresponding author: sumitkrmgr@gmail.com;* ORCID: https://orcid.org/0000-0002-5695-5944

Received: 11 October 2023; revised: 31 December 2023; accepted: 10 January 2024

ABSTRACT

SARS-CoV-2, the virus responsible for the COVID-19 pandemic, is highly contagious and has caused widespread loss of life. In the quest to find effective antiviral agents, attention has turned to oxadiazole derivatives, which are known for their potential antiviral properties in such as CoViTris2020, ChloViD2020, *etc*. To evaluate their effectiveness, molecular docking and molecular dynamics simulations are conducted for various oxadiazole derivative in interactions with critical proteins involved in the viral infection process. These proteins encompass transmembrane-serine-2 (TMPRSS2), 3-chymotrypsin-like-protease (3CLpro), angiotensin-converting-enzyme-2 (ACE2), and papain-like-protease (PLpro). The study shows that the oxadiazole derivatives exhibited their most stable complexes when interacting with TMPRSS2 in comparison to 3CLpro, ACE2, and PLpro. In particular, Oxa8 displayed a binding energy of -6.5269 kcal/mol with TMPRSS2. In contrast, the binding energies with ACE2, 3CLpro, and PLpro were -5.74, -4.56, and -5.56 kcal/mol, respectively. RMSD analysis during MD simulations demonstrated that the complex structure remained consistently stable. During the initial 2 ns, the RMSD value for the ligand concerning its interaction with the protein backbone hovered around 2 Å, indicating a sustained level of structural stability. In conclusion, this study suggests that oxadiazole derivative Oxa8 holds promise as a potential inhibitor of SARS-CoV-2, particularly due to its strong binding affinity with TMPRSS2 and its enduring structural stability observed in molecular dynamics simulations.

Keywords: COVID-19; Oxadiazole; transmembrane-serine; 3-chymotrypsin-like-protease; angiotensin-converting-enzyme

INTRODUCTION

Corona virus 2 (SARS-CoV-2) is a contagious and caused form submicroscopic infectious agent virus [1-3]. The Covid-19 disease has been announced as pandemic by world health organization due to catastrophe of deaths reported. Over 750 million cases of Covid-19 reported, which includes more than 6 million deaths. Therefore, it is prime interest for eminent scientist to prepare drugs having novel antivirals activity against Covid-19 [4].

Oxadiazole derivatives are majorly used for antiviral activities due to its important properties. CoViTris2020 (1,2,3-tris[5-(3,4,5-trihydroxyphenyl)-1,3,4-oxadiazol-2-yl]propan-2-ol) and ChloViD2020 (5-[5-(7-chloro-4-hydroxyquinolin-3-yl)-1,3,4-oxadiazol-2-yl]benzene-1,2,3-triol) are some examples of oxadiazole derivatives [5, 6]. Apart from its antiviral properties, Because of their numerous biological actions, oxadiazole derivatives have been explored for their potential therapeutic usefulness in a variety of scenarios [7-11]. They have the ability to suppress the growth of a variety of bacteria by targeting specific enzymes or biological processes. Some oxadiazole compounds have been shown to be cytotoxic to cancer cells. They have the ability to limit tumour growth by interfering with cell division, inducing apoptosis (programmed cell death), and interfering with cell division [12]. The potential of these compounds as chemotherapeutic agents is being investigated. They may block inflammatory pathways and lower pro-inflammatory molecule production, potentially providing relief for a variety of inflammatory disorders. Certain oxadiazole derivatives exhibit antioxidant activity, which means they can aid in the neutralization of damaging reactive oxygen species (ROS) and the protection of cells from oxidative stress. This feature is relevant to a variety of disorders associated with oxidative damage. Oxadiazole derivatives have been studied for their capacity to shield brain cells from injury, perhaps making them effective in the treatment of neurodegenerative illnesses such as Alzheimer's and Parkinson's [13, 14]. Some derivatives have demonstrated cardiovascular

effects, such as vasodilation (blood vessel widening) and possible utility in the treatment of cardiovascular problems.

SARS-CoV-2, the virus responsible for COVID-19, utilizes a fusion protein consisting of two primary subunits, S1 and S2, for its transmission and entry into host cells [2, 3, 15]. The initial step involves the interaction between the viral spike protein and the angiotensin-converting enzyme 2 (ACE2), which is pivotal for determining viral entry [2, 16]. Subsequently, the transmembrane serine protease 2 (TMPRSS2) cleaves the spike protein into smaller subunits, facilitating the virus's entry into host cells by allowing access to the infectious viral RNA. Once inside the host cell, SARS-CoV-2 employs two essential proteases, namely the 3-chymotrypsin-like protease (3CLpro, also known as the main protease or Mpro) and the papain-like protease (PLpro) [2, 16]. These proteases play a crucial role in breaking down polyproteins, releasing 16 non-structural proteins (nsps). These nsps are vital for viral replication and transcription, ultimately leading to the production of viral genomes through the accumulation of infectious replicase on the host cell membrane [2, 16].

In the current study, a series of various substituted oxadiazoles have been studied as a precursor for multi-targeted inhibitors against SARS-CoV-2 through molecular docking and detailed quantum chemical calculation to understand the effect of substitution. These precursors are angiotensin-converting enzyme 2 (ACE2), transmembrane serine protease 2 (TMPRSS2), 3-chymotrypsin-like protease (3CLpro, also known as the main protease or Mpro) and the papain-like protease (PLpro). The molecular dynamics study has also been performed to understand important physiological parameters to predict the real mode of interactions of oxadiazole derivative with precursors of SARS-CoV-2.

Computational details

Structural detail: Various derivatives of oxadiazole have been taken for the computational calculation. These derivatives contain hydrogen (H), carbon (C), oxygen (O) and nitrogen (N) [17, 18]. Fig. 1 shows the chemical structure of 1,3,4-oxadiazole derivative. In this structure, R_1 and R_2 are supplanted by various substituent groups such as methyl ($-CH_3$), ethyl($-C_2H_5$), propyl ($-C_3H_7$), hydroxyethyl($-C_2H_5OH$), chloroethyl ($-C_2H_5-Cl$), carboxyethyl ($-C_2H_5-COOH$) and thioethyl ($-C_2H_5-SH$) and aminoethyl ($C_2H_5-NH_2$). There substituents have either electron withdrawing or electron donating properties.

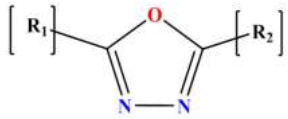

Fig. 1. Chemical structure of 1, 3, 4 oxadiazole derivatives having substituents R_1 and R_2

Fig. 2 depicts the chemical structures of nine derivatives of 1,3,4-oxadiazole having either electron withdrawing or electron donating substituents. These structures are names as Oxa1, Oxa2, Oxa3, Oxa4, Oxa5, Oxa6, Oxa7, Oxa8 and Oxa9 whereas the chemical structure of these compounds is indicated in the figure.

Molecular docking: Interaction of ligand and receptor has been studied using the implement of molecular docking. It dictates the ligand-receptor binding occurs through various non-covalent interaction between protein and ligand. Some useful software is used for docking. AutoGrid4, AutoDock4 and python programming tools are used for the study of oxadiazole with various precursors of SARS-CoV-2 [15].

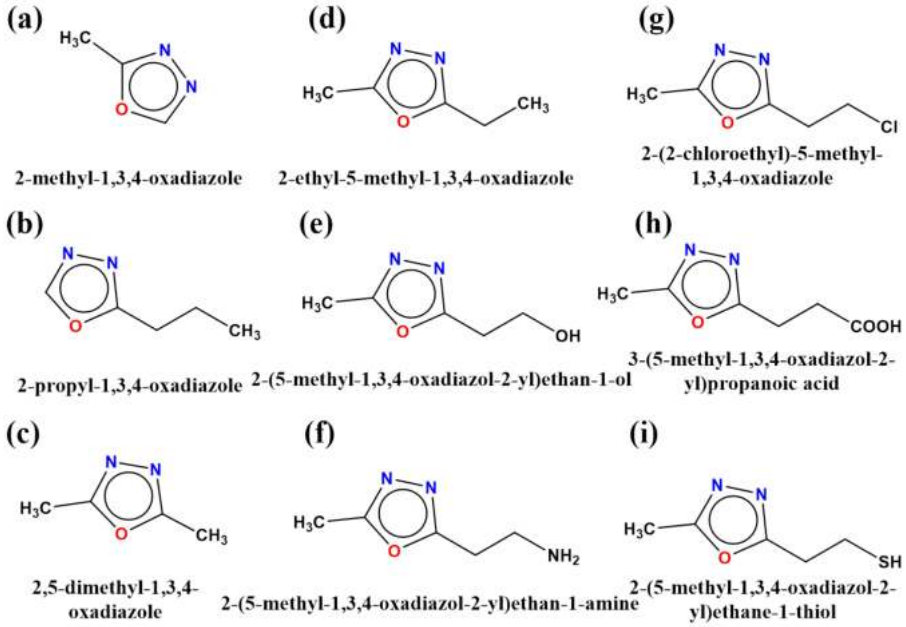

Fig. 2. Structures of derivatives of 1,3,4-oxadiazole as shown in (a)-(i). These structures are names as Oxa1-9

Molecular dynamics simulation: To explain the structural properties of oxadiazole derivatives with a precursor of SARS-CoV-2, the calculation using molecular dynamics simulation through Gromacs program package 2022 [19]. The simulations used the CHARMM27 force field, which includes the specific arrangement to encounter the dihedral potential terms [20, 21]. The force field uses the classical TIP3P model considering the Lennard-Jones interaction. The potential for these simulations is applicable for all atom force field for protein. These proteins are homogenously solvated in the form of a cubic box having each point charge models water molecule. Periodic boundary conditions are applied to get rid of unnecessary boundary effect whereas proper number of counter ions have been added for neutralization of the system. The algorithm is used to solve the linear constraint to maintain the different bond lengths combining hydrogen bonds. Constant number of particles, volume and temperature (NVT) ensemble is prepared to perform the simulation at 300 K applying the Berendsen temperature coupling followed by NPT ensemble including pressure in place of temperature through Parrinello-Rahman pressure coupling method using constant of 0.1 ps and 1 bar pressure. The short-range electrostatic and van der Waals cutoff radii are chosen 1.2 nm. The time step used for the simulation is 1fs whereas 0.16 nm is used as Fourier spacing during simulation. MD simulation is performed for 2ns and after every 10ps, the coordinates during the simulation is saved for the analysis.

RESULTS AND DISCUSSIONS

The docking study has been performed each oxadiazoles with transmembrane serene-2 (TMPRSS2), 3-Chymotrypsin-like protease (3CLpro), angiotensin-converting enzyme 2 (ACE2) and papain-like protease (PLpro). The PDB IDs for these proteins are 1Z8A, 3AW0, 3D0G, and 3E9S, respectively. Energetically the most stable complexes of oxadiazole derivatives with respect to binding pockets of TMPRSS2, 3CLpro, ACE2 and PLpro are studied to understand the amino acids involved during interactions and reported in Table 1.

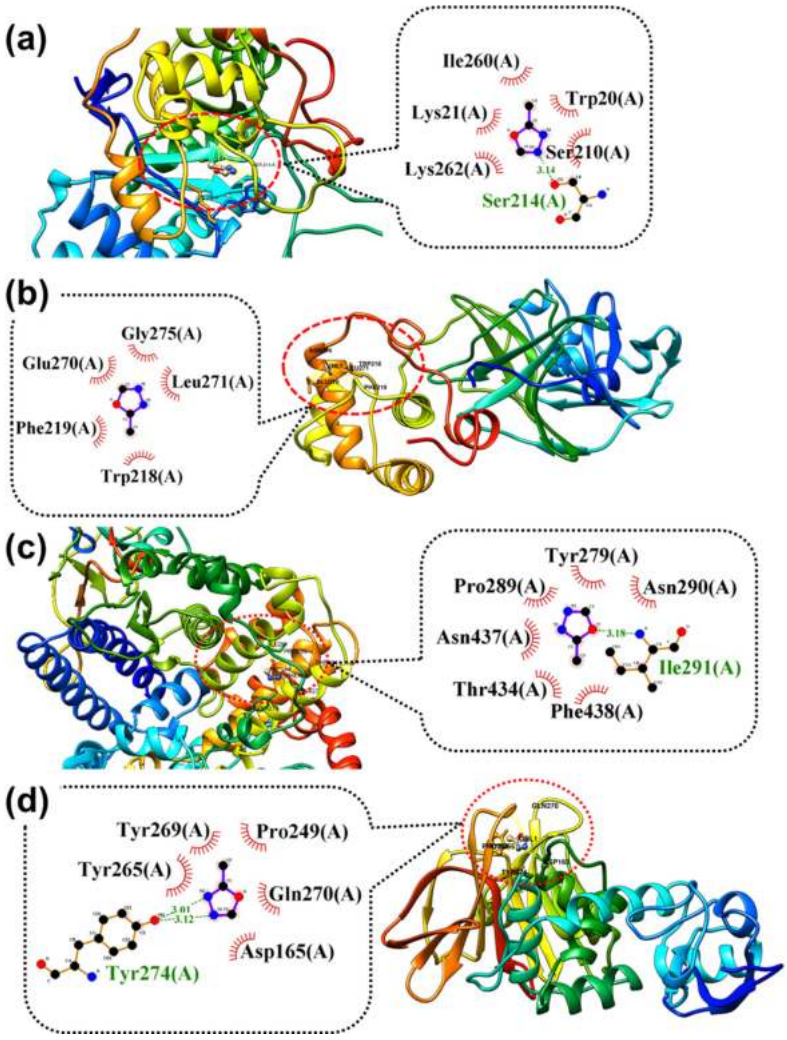

Fig. 3. Lowest binding energy docking pose of Oxa1 in (a) transmembrane serine protease 2 (TMPRSS2) PDB ID: 1Z8A, (b) angiotensin-converting enzyme 2 (ACE2) PDB ID: 3D0G, (c) 3-chymotrypsin-like protease (3CLpro) PDB ID: 3AW0 and (d) papain–like protease (PLpro) PDB ID: 3E9S. Individual ligand-complex docking site has been highlighted by red dotted circle whereas underlying specific amino acids are indicated by black dotted rectangle

Oxa1 against SARS-CoV-2: The interaction of Oxa1 to the binding pockets of TMPRSS2, 3CLpro, ACE2 and PLpro is investigated and reported in Fig. 3. Oxa1 interacts with chain A of TMPRSS2 through amino acid Ile260, Lys21, Trp20, Lys262, Ser210 and Ser214. Mainly, it includes the major H-bonding distances of 3.05 and 2.92Å with Lys21 and Ser210, respectively. The hydrophobic interaction with Tyr209 is found at 3.95Å. Oxa1 interacts with chain A of 3CLpro through amino acid Gly275, Leu271, Glu270, Phe219, Trp218. The H-bonding distance is 2.98Å with Glu270. The hydrophobic interactions are 3.37, 3.90, 3.91, 3.90Å with Trp218, Glu270, Leu271, Asn274, respectively. Chain A of ACE2 through amino acid Tyr279, Pro289, Asn290, Asn437, Thr434, Phe438, and Ile291 interact with Oxa1. Hydrogen bonding distances are 2.17, 2.19, 3.19, 2.50Å with Tyr279, Pro289, Ile291, respectively. These hydrogen bonding are also responsible for the stability of various molecular system [22-26]. Hydrophobic interactions of 3.79 and 3.85Å are measured with Ile291 and Asn473, respectively. Oxa1 interact with chain A of PLpro through amino acid Pro249, Tyr269, Tyr265, Gln270, Asp165, Tyr274 the major H-bonding distances are 2.03, 2.89, 2.49, 2.69, 2.13, 2.26 and 2.44, 2.39Å with Trp107, Asn110, Tyr113, Ser115, Ser116, Tyr274 with Gln270, Tyr274. The hydrophobic interactions with a distance of 3.86 and 3.78Å form with Pro249 and Tyr265, respectively.

Oxa2 against SARS-CoV-2: Oxa2 engages with chain A of TMPRSS2 by forming interactions with specific amino acids, including Ser210, Leu212, Pro211, Lys262, Lys21, Asp216, Ser214, and Trp20. Among these, notable hydrogen bonding distances are observed at 3.09, 2.35, and 3.54 angstroms with Lys21, Ser210, and Lys262. Furthermore, hydrophobic interactions are established at distances of 3.67 and 3.70 angstroms with Leu212 and Lys262. In its interaction with chain A of 3CLpro, Oxa2 interacts through amino acids Leu271, Asn274, Gly275, Trp218, Phe219, Glu270, and Leu220. A significant hydrogen bond is formed at a distance of 2.81 angstroms with Leu220, while hydrophobic interactions occur at distances of 3.67, 3.79, 3.72, and

Table 1. Amino acids involved during the important interactions of oxadiazole derivatives

Ligand	Substrate	Amino acids
Oxa1	1Z8A	Ile260a, Lys21a, Trp20a, Ser210a
	3AW0	Gly275a, Glu270a, Leu271a, Phe219a, Trp218a
	3D0G	Tyr279a, Pro289a, Asn437a, Thr434a, Phe438a, Ile291a
	3E9S	Pro249a, Tyr269a, Gln270a, Asp165a
Oxa2	1Z8A	Ser210a, Leu212a, Pro211a, Lys262a, Asp216a, Ser214a, Trp20a
	3AW0	Leu271a, Asn274a, Gly275a, Glu270a, Trp218a, Phe219a, Leu220a
	3D0G	Phe438a, Pro289a, Asn437, Ile291a, Tyr279a
	3E9S	Leu163a, Tyr269a, Thr302a, Pro249a, Gln270a, Asp165a, Gly164a
Oxa3	1Z8A	Ser210a, Tyr209a, Trp20a, Lys262, Ile260a, Asp216a
	3AW0	Phe219a, Trp218, Leu271a, Glu270a
	3D0G	Tyr83a, Leu79a, Phe28a, Leu472e, Asn473e, Tyr475e
	3E9S	Thr302a, Tyr265a, Gln270a, Gly164a, Tyr274a, Asp165a, Tyr269a
Oxa4	1Z8A	Ile260a, Ser210a, Trp20a, Ser214a, Tyr209a, Lys21a, Asp216, Lys262a
	3AW0	Arg279, Leu271, Glu270a, Phe219a, Trp218a
	3D0G	Pro500a, Asp499a, Phe452a, Trp477a, Trp271a, Arg169, Lys481a, Trp478a, Trp165a, Ala264a
	3E9S	Thr302a, Tyr269a, Leu163a, Tyr265a, Gly164a, Gln270a, Asp165a, Tyr274a
Oxa5	1Z8A	Gly18a, Ile260a, Asp216a, Ser210a, Ser214a, Lys21a, Trp20a, Lys262a
	3AW0	His41, Met49a, Ile188a, Thr190a, Gln189a, Met165a, Glu166a, Asp177a
	3D0G	Leu79a, Tyr83a, Asn473e, Tyr475e, Leu472e, Ala471e, Cys474e
	3E9S	Arg167a, Met209a, Thr302a, Asp165a, Tyr265a, Tyr274a, Asp303a, Ser246a, Ala247a
Oxa6	1Z8A	Ile260a, Gly18a, Ser210a, Lys21a, Ser214a, Asp216a, Trp20a, Lys262a
	3AW0	Asp187a, Met49a, Thr190a, Gln189a, Ile188a, Gln192a, Glu166a, Met165a
	3D0G	Tyr83a, Leu79a Asn473e, Tyr475e, Leu472e, Ala471e
	3E9S	Arg167a, Thr302a, Tyr274a, Tyr269a, Tyr265a, Asp165a, Met209a, Ala247a, Ser246a, Asp303a
Oxa7	1Z8A	Ser210a, Trp20a, Asp216a, Ser214a, Lys21a, Lys262a, Tyr209a, Ile260a
	3AW0	Gln192a, Thr190a, Gln189a, Asp187a, Met49a, Glu166a, Met165a, Ile188a
	3D0G	Pro500a, Trp477a, Arg169a, Trp478a, Asp499a, Ala264a, Lys481a, Trp165a, Phe452a, Trp271a
	3E9S	Gln270a, Gly164a, Tyr269a, Thr302a, Tyr264a, Tyr265a, Asp165a
Oxa8	1Z8A	Lys77a, Tyr48a, Tyr209a, Ser210a, Trp20a Lys21a, Ser214a, Asp216a, Lys262a, Gln183a, Ile260a, Asp43a
	3AW0	Asp153a, Ile106a, Thr111a, Gln110a, Thr292a, Asp295a, Phe294a, Asn151a
	3D0G	Tyr83a, Leu79a, Phe28a, Tyr475e, Leu472e, Cys474e
	3E9S	Phe70a, Ala69a, Arg66a, Thr75a, Phe80a, Tyr73a, Leu81a, Glu78a, Pro60a, Asp77a
Oxa9	1Z8A	Gln183a, Tyr48a, Tyr209a, Trp20a, Lys21a, Ser214a, Asp216a, Ser210a, Lys262a, Ile260a
	3AW0	Val104a, Ile160a, Thr111a, Asp295a, Phe294a, Asn151a, Gln110a, Ser158a
	3D0G	Asn290a, Asn437a, Thr434a, Tyr279a, Phe438a, Lys441a, Asp292a, Ile291a, Pro289a
	3E9S	Tyr269a, Gly164a, Gln270a, Leu163a, Tyr274a, Tyr265a, Asp165a

3.76 angstroms with Trp218, Glu270, Leu271, and Asn274, respectively. When interacting with chain A of ACE2, Oxa2 utilizes amino acids Phe438, Ile291, Pro289, Tyr279, and Asn437. Noteworthy hydrogen bonding interactions are established at distances of 2.89, 2.67, and 2.54 angstroms with Tyr279, Lys288, and Asn437, respectively. Additionally, a hydrophobic interaction is observed at a distance of 3.82 angstroms with Phe438. In its interaction with chain A of PLpro, Oxa2 forms connections through amino acids Leu163, Gly164, Tyr269, Asp165, Tyr265, Thr302, Pro249, Gln270, and Tyr274. The major hydrogen bonding distances include 2.67 and 2.54 angstroms with Lys288 and Asn43, respectively. Furthermore, a hydrophobic interaction is observed at a distance of 3.82 angstroms with Phe438. **Fig. S1** in the supporting information represents the aforementioned interaction.

Oxa3 against SARS-CoV-2: Oxa3 establishes specific interactions with Chain A of various proteins, leading to significant molecular bonding and hydrophobic associations. In its interaction with Chain A of TMPRSS2, Oxa3 engages amino acids Ser210, Tyr209, Ile260, Trp20, Lys21, Lys262, Ser214, and Asp216. Notably, it forms hydrogen bonds, with distances of 3.02, 2.44, and 3.36Å, with Lys21, Ser210, and Lys262, respectively. Additionally, hydrophobic interactions occur at distances of 3.88 and 3.86Å with Tyr209 and Lys262, respectively. Oxa3 interacts with Chain A of 3CLpro through amino acids Phe219, Trp218, Glu270, and Leu271. A significant hydrogen bond is established at a distance of 2.95Å with Leu220, while hydrophobic interactions take place at a distance of 3.73Å with Leu271. Its binding to Chain A of ACE2 involves amino acids Leu472, Asn473, Tyr83, Leu79, Tyr475, and Phe28. Notably, Asn473 participates in a hydrogen bond at a distance of 2.13Å. Furthermore, hydrophobic interactions are observed with Leu79, Tyr83, and Leu472, occurring at distances of 3.74, 3.67, and 3.59Å, respectively. Oxa3 interacts with Chain A of PLpro, where key hydrogen bonding distances of 2.03, 2.89, 2.49, 2.69, 2.13, 2.26, 3.56, 2.33, and 1.89Å are noted with Trp107, Asn110, Tyr113, Ser115, Ser116, Tyr274, Tyr265, Gln270, and Tyr274, respectively. Additionally, hydrophobic interactions occur at distances of 3.87, 3.70, and 3.59Å with Asp165, Tyr265, and Thr302, respectively. **Fig. S2** shows various interaction with precursors of SARS-CoV-2. In these interactions, Oxa3 forms both hydrogen bonds and hydrophobic contacts with specific amino acids within the target proteins, which play a critical role in their binding and potential functional outcomes.

Oxa4 against SARS-CoV-2: Oxa4 engages in specific interactions with Chain A of various proteins, fostering molecular bonds and hydrophobic associations. In its interaction with Chain A of TMPRSS2, Oxa4 binds to amino acids Ile260, Ser210, Trp20, Ser214, Tyr209, Lys21, Asp216, and Lys262. It notably forms hydrogen bonds, with distances measuring 3.06, 2.41, and 3.46Å, with Lys21, Ser210, and Lys262, respectively. Additionally, a hydrophobic interaction occurs at a distance of 3.82Å with Lys262. Oxa4 interacts with Chain A of 3CLpro through amino acids Arg279, Trp218, Leu271, Phe219, and Glu270. A prominent hydrophobic interaction takes place, with a distance of approximately 3.74Å, involving Trp218 and Leu271. Its binding to Chain A of ACE2 involves amino acids Pro500, Asp499, Phe452, Trp477, Trp271, Arg169, Lys481, Trp165, Ala264, and Trp478. Notably, Oxa4 forms hydrogen bonds at distances of 2.16, 3.26, and 2.49Å with Arg169, Trp477, and Lys481, respectively. Furthermore, it engages in hydrophobic interactions at distances of 3.77, 3.81, 3.47, 3.98, 3.64, and 3.71Å with Trp165, Ala264, Phe452, Leu456, Trp477, and Trp478, respectively. Oxa4 also interacts with Chain A of PLpro through amino acids Thr302, Tyr269, Leu163, Tyr265, Tyr274, Gly164, Gln270, and Asp165. **Fig. S3** shows various interaction with precursors of SARS-CoV-2. In these interactions, Oxa4 establishes hydrogen bonds and hydrophobic contacts with specific amino acids within the target proteins, which play a crucial role in their binding and potential functional effects.

Oxa5 against SARS-CoV-2: Oxa5 establishes specific interactions with Chain A of various proteins, facilitating molecular bonding and hydrophobic associations. In its interaction with Chain A of TMPRSS2, Oxa5 binds to amino acids Gly18, Ile260, Asp216, Lys262, Ser210, Ser214, Trp20, and Lys21. Notably, it forms hydrogen bonds at distances of 2.90, 2.25, 3.11, 2.32, and 3.43Å with Thr19, Trp20, Lys21, Ser210, and Lys262, respectively. Additionally, a hydrophobic interaction occurs at a distance of 3.89Å with Lys262. Oxa5 interacts with Chain A of 3CLpro through amino acids His41, Met49, Asp187, Ile188, Glu166, Thr190, Gln189, and Met165. Key hydrogen bonds are established at distances of 2.89, 2.47, and 2.08Å with Ile188, Gln189, and Thr190, respectively. Furthermore, it engages in a hydrophobic interaction at a distance of 3.96Å with ASP187. Its binding to Chain A and Chain E of ACE2 involves amino acids Asn473, Leu79, Tyr475, Ala471, Cys474, Tyr83, and Leu472. Notably, Oxa5 forms crucial hydrogen bonds at distances of 2.08 and 1.89Å with Asn473 and Cys474, respectively. Additionally, it engages in hydrophobic interactions at distances of 3.71, 3.76, 3.53, and 3.95Å with Leu79, Tyr83, Leu472, and Tyr475, respectively. Oxa5 also interacts with Chain A of PLpro (PDB ID: 3e9s) through amino acids Arg167, Ala247, Met209, Ser246, Asp165, Thr302, Tyr265, Tyr274, and Asp303. Major hydrogen bonding distances are 3.44, 2.30, and 2.33Å with Ser246, Ala247, and Tyr274, respectively. Furthermore, it engages in hydrophobic interactions at distances of 3.88 and 3.56Å with Arg167 and Tyr265, respectively. **Fig. S4** shows various interaction with precursors of SARS-CoV-2. In these interactions, Oxa5 establishes hydrogen bonds and hydrophobic contacts with specific amino acids within the target proteins, contributing to their binding and potential functional effects.

Oxa6 against SARS-CoV-2: Oxa6 exhibits distinct interactions with various proteins in chain A of different target molecules. These interactions involve specific amino acids and are characterized by varying hydrogen bonding distances and hydrophobic interactions. Oxa6 engages with TMPRSS2 through amino acids Ile260, Gly18, Lys262, Ser210, Lys21, Ser214, Asp216, and Trp20. Notably, major hydrogen bonding occurs at distances of 3.03, 2.36, 3.04, 2.44, and 3.33 angstroms (Å) with Thr19, Trp20, Lys21, Ser210, and Lys262, respectively. Additionally, a hydrophobic interaction is observed at a distance of 3.89Å with Lys262. Oxa6 forms interactions with 3CLpro via amino acids Asp187, Met149, Thr190, Gln189, Ile188, Gln192, Glu166, and Met165. The primary hydrogen bonding distance is 1.91Å with Thr190. Furthermore, a hydrophobic interaction is detected at a distance of 3.91Å with Asp187. Oxa6 interacts with both chains A and E of ACE2 involving amino acids Tyr83, Asn473, Tyr475, Ala471, Leu472, and Leu79. Key hydrogen bonding distances are 2.19, 2.06, and 2.38Å with Ala471 and Asn473. Additionally, hydrophobic interactions are observed at distances of 3.98Å with Leu79 and 3.89Å with Tyr475. Oxa6 establishes interactions with PLpro through amino acids Asp303, Ser246, Arg167, Ala247, Thr302, Tyr274, Tyr269, Tyr265, Asp165, and Met209. Notably, hydrogen bonding distances are found to be 2.03, 2.89, 2.49, 2.69, 2.13, and 2.26Å with Trp107, Asn110, Tyr113, Ser115, Ser116, and Tyr174, respectively. Additionally, hydrophobic interactions occur at distances of 3.74Å with Tyr265 and 3.89Å with Tyr269. **Fig. S5** shows various interaction with precursors of SARS-CoV-2. These interactions provide valuable insights into the binding of Oxa6 with its respective protein targets, shedding light on potential molecular mechanisms and therapeutic implications.

Oxa7 against SARS-CoV-2: Oxa7 engages in specific interactions with various proteins within Chain A of different target molecules. These interactions involve distinct amino acids and are characterized by varying hydrogen bonding distances and hydrophobic interactions. Oxa7 forms interactions with TMPRSS2

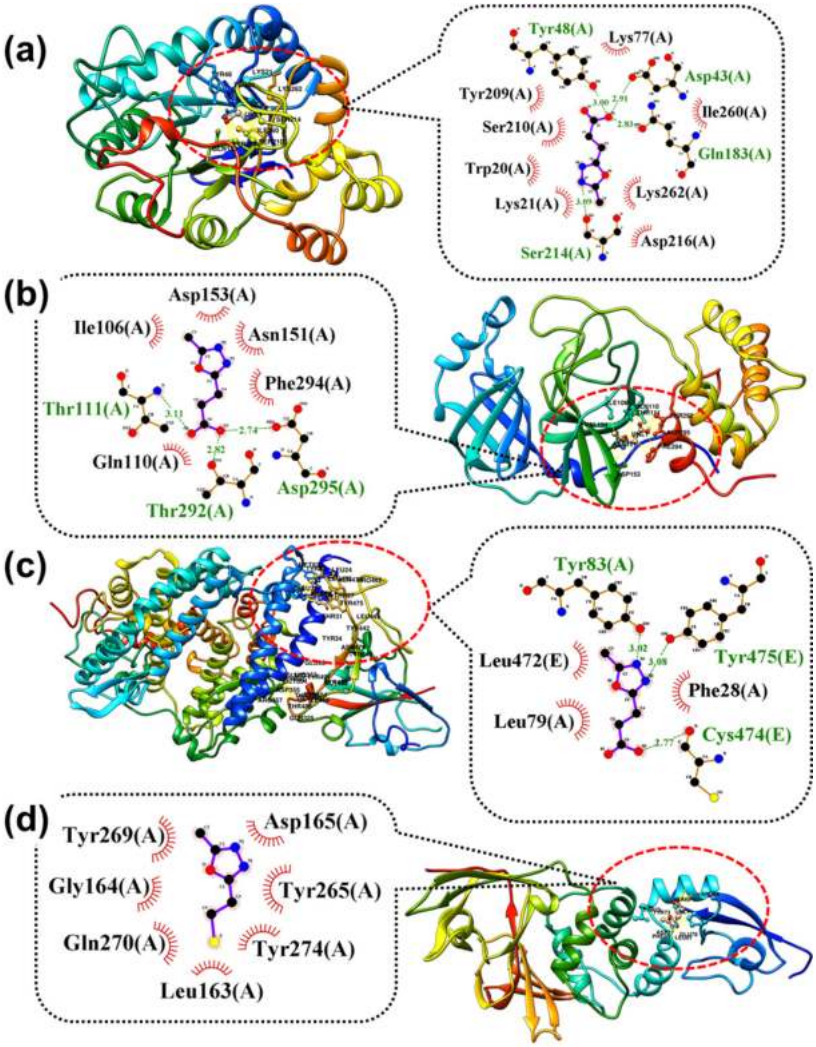

Fig. 4. Lowest binding energy docking pose of Oxa8 in the (a) transmembrane serine protease 2(TMPRSS2) PDB ID: 1Z8A, (b) angiotensin-converting enzyme 2 (ACE 2) PDB ID: 3D0G, (C) 3-chymotrypsin-like protease (3CLpro) PDB ID: 3AW0 and (papain-like protease (PLpro) PDB ID: 3E9S. Individual ligand-complex docking site has been highlighted by red dotted circle whereas underlying specific amino acids are indicated by black dotted rectangle

via amino acids Ser210, Trp20, Asp216, Ser214, Ile260, Tyr209, Lys262, and Lys21. Notably, major hydrogen bonding occurs at distances of 3.04Å with Lys21, 2.44Å with Ser210, and 3.47Å with Lys262. Additionally, a hydrophobic interaction is observed at a distance of 3.74Å with Asp187. Oxa7 interacts with 3CLpro through amino acids Gln192, Ile188, Thr190, Gln189, Asp187, Met49, Glu166, and Met165. The primary hydrogen bonding distances are found to be 3.00Å with Ile188 and 2.66Å with Gln189. Furthermore, a hydrophobic interaction is detected at a distance of 3.83Å with Asp187. Oxa7 establishes interactions with Chain A of ACE2 involving amino acids Pro500, Trp271, Arg169, Trp478, Asp499, Ala264, Lys481, Trp165, Phe452, and Trp477. Key hydrogen bonding distances are found to be 2.21Å with Arg169, 3.39Å with Trp271, 3.12Å with Trp477, and 2.42Å with Lys481. Additionally, hydrophobic interactions are observed at distances of 3.75Å with Trp165, 3.63Å with Ala264, and 3.64Å with Trp478. Oxa7 interacts with Chain A of PLpro through amino acids Gln270, Gly164, Tyr269, Thr302, Asp165, Tyr265, and Tyr274. The hydrogen bonding distances are found to be 2.53Å with Gln270 and 1.91Å with Tyr274. Additionally, hydrophobic interactions occur at distances of 3.64Å with Tyr265 and 3.39Å with Thr302. **Fig. S6** shows various interaction with precursors of SARS-CoV-2. These interactions provide valuable insights into the binding of Oxa7 with its respective protein targets, contributing to a better understanding of potential molecular mechanisms and therapeutic implications.

Oxa8 against SARS-CoV-2: The Lowest binding energy docking pose of oxa8 in the TMPRSS2, ACE 2, 3CLpro and PLpro is reported in Fig. 4. Here, Oxa8 establishes unique interactions with various proteins within Chain A of different target molecules. These interactions involve specific amino acids and are characterized by varying hydrogen bonding distances and hydrophobic interactions. Oxa8 engages TMPRSS2 through amino acids Tyr209, Tyr48, Lys77, Asp43, Ser210, Trp20, Lys21, Ser214, Asp216, Lys262, Gln183, and Ile260. Notably, major hydrogen bonding occurs at distances of 3.02, 3.44, 2.87, 2.13, 2.44, and 3.45 angstroms (Å) with Lys21, Tyr48, Lys77, Gln183, Ser210, and Lys262, respectively.

Additionally, a hydrophobic interaction is observed at a distance of 3.84Å with Lys262. Oxa8 interacts with 3CLpro via amino acids Asp153, Ile106, Asn151, Phe294, Thr111, Gln110, Thr292, and Asp295. The primary hydrogen bonding distances are found to be 2.72Å with Gln110, 2.16Å with Thr111, 2.60Å with Asp153, and 3.07Å with ASP295. Furthermore, hydrophobic interactions occur at distances of 3.92Å with Val104, 3.56Å with Ile106, 3.85Å with Thr292, and 3.62Å with PHE294. Oxa8 establishes interactions with both chains A and E of ACE2 involving amino acids Tyr83, Leu79, Phe28, and Tyr475, Leu472, and Cys474. Key hydrogen bonding distances are found to be 2.12Å with Ala471, 2.20Å with Asn473, and 2.88Å with Cys474. Additionally, hydrophobic interactions are calculated with Phe28, Leu79, Tyr83, Leu472, and Tyr475. Oxa8 interacts with Chain A of PLpro through amino acids Phe70, Ala69, Arg66, Thr75, Phe80, Tyr73, Leu81, Glu78, Pro60, and Asp77.

The major hydrogen bonding distances are found to be 2.03, 2.89, 2.49, 2.69, 2.13, and 2.26Å with Trp107, Asn110, Tyr113, Ser115, Ser116, and Tyr274, respectively. Additionally, hydrophobic interactions occur at distances of 3.70Å with Arg66, 3.90Å with Ala69, 3.65Å with Tyr73, 3.68Å with Phe80, and 3.64Å with Leu81. These interactions provide valuable insights into the binding of Oxa8 with its respective protein targets, offering a comprehensive understanding of potential molecular mechanisms and therapeutic implications.

Oxa9 against SARS-CoV-2: Oxa9 exhibits distinct binding interactions with Chain A of various proteins, each characterized by specific amino acids and varying hydrogen bonding distances as well as hydrophobic interactions. Oxa9 forms interactions with TMPRSS2 via amino acids Gln183, Tyr48, Tyr209, Trp20, Lys21, Ser214, Asp216, Ser210, Lys262, and Ile260. Notably, major hydrogen bonding occurs at distances of 2.99Å with Lys21, 2.49Å with Ser210, and 3.34Å with Lys262. Additionally, a hydrophobic interaction is observed at a distance of 3.82Å with Lys262. Oxa9 interacts with 3CLpro via amino acids Val104, Ile106, Thr111, Asp295, Ser158, Gln110, Asn151, and Phe294. The primary hydrogen bonding distance is found to be 3.36Å with Gln110. Furthermore, a hydrophobic interaction occurs at a distance of 3.60Å with Phe294. Oxa9 establishes interactions with Chain A of ACE2, involving amino acids Asn290, Asn437, Tyr279, Thr434, Asn437, Pro289, Phe438, Ile291, and Asp292. Key hydrogen bonding distances are found to be 2.10Å with Tyr279, 2.98Å with Pro289, and 2.52Å with Ile291. Additionally, hydrophobic interactions are observed at distances of 3.83Å with Ile291 and 3.75Å with Asn437. Oxa9 interacts with Chain A of PLpro through amino acids Tyr269, Gly164, Gln270, Leu163, Tyr274, Tyr265, and Asp165. The major hydrogen bonding distances are found to be 2.03Å with Trp107, 2.89Å with Asn110, 2.49Å with Tyr113, 2.69Å with Ser115, 2.13Å with Ser116, and 2.26Å with Tyr274. Additionally, hydrophobic interactions occur at distances of 3.72Å with Asp165, 3.75Å with Tyr265, 3.63Å with Tyr269, and 3.95Å with Gln270. **Fig. S7** shows various interaction with precursors of SARS-CoV-2. These interactions provide valuable insights into the binding of Oxa9 with its respective protein targets, shedding light on potential molecular mechanisms and therapeutic implications.

Interaction energies: The binding energies of oxadiazole derivatives with various precursors of Precursors of SARS-CoV-2 has been calculated and shown in the Table 2. The study shows that the binding energies for each oxadiazoles with TMPRSS2 is calculated lowest in comparison to 3-Chymotrypsin-

Table 2. Binding energy (in kcal/mol) of oxadiazole derivatives (1-9) with four precursors of SARS-CoV-2

Ligand	Precursors of SARS-CoV-2			
	TMPRSS2 (PDB ID: 1Z8A)	ACE2 (PDB ID: 3D0G)	3CLpro (PDB ID: 3AW0)	PLpro (PDB ID: 3E9S)
Oxa1	**-4.23**	-3.85	-3.18	-3.90
Oxa2	**-5.11**	-4.55	-3.88	-4.74
Oxa3	**-4.96**	-4.74	-3.48	-4.51
Oxa4	**-5.31**	-5.56	-3.68	-5.10
Oxa5	**-5.60**	-5.46	-4.10	-4.99
Oxa6	**-5.64**	-4.97	-4.40	-4.90
Oxa7	**-5.57**	-5.23	-3.91	-5.23
Oxa8	**-6.53**	**-5.75**	**-4.56**	**-5.56**
Oxa9	**-5.19**	-4.44	-3.59	-4.66

like protease (3CLpro), angiotensin-converting enzyme 2 (ACE2) and papain-like protease (PLpro). The binding energy of the most stable complex of Oxa1 with TMPRSS2 is -4.23 kcal/mol whereas that with ACE2, 3CLpro and PLpro are -3.84, -3.18, and -3.90 kcal/mol, respectively. The binding energies for each of the oxadiazole with all the precursors are plotted in the Fig. 5. A careful observation of these data shows that the oxadiazole derivative, oxa8, has the highest binding energy of the complexes among all derivatives whereas the lowest binding energy of the complexes are found for Oxa1. Therefore, the molecular dynamics simulation has been studied for Oxa8 with TMPRSS2.

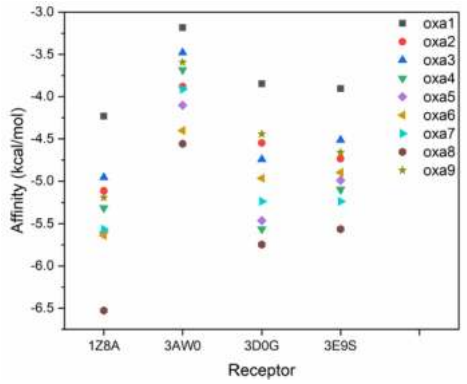

Fig. 5. Binding affinities of oxadiazole derivatives (1-9)

Molecular dynamics simulation: Root mean square deviation (RMSD) is a critical statistic for understanding the protein's backbone structure evolves throughout simulation from its starting conformation to its end location [27]. This value gives useful information on the protein's stability in terms of conformational changes. Essentially, the fewer the detected RMSD deviations resembles with maximizing the stable the protein's structure. The stability of oxadiazole derivative with transmembrane serine protease 2(TMPRSS2) PDB ID: 1Z8A precursor of SARS-CoV-2 has been calculated by conducting the RMSD calculations for the protein as well as backbone for 2 ns simulation period (Fig. 6a) [28]. The results from the RMSD analysis revealed a much smother patterns for the complex after a simulation time of 0.6 ns.

The RMSD value for ligand with respect to backbone of about 2Å for initial 2 ns exhibited a sustained level of stability.

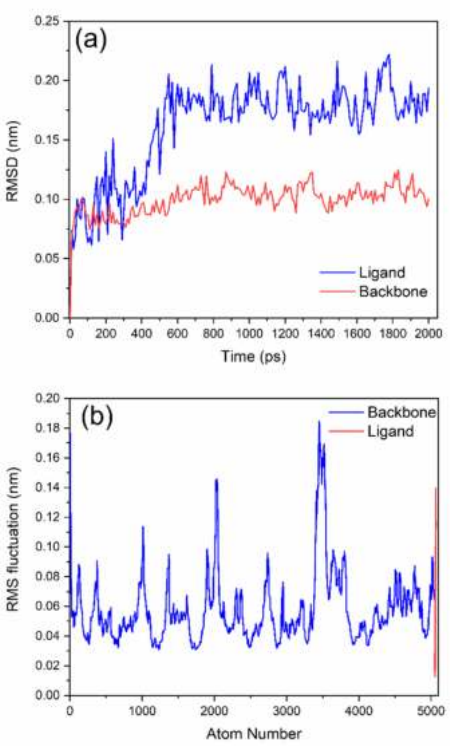

Fig. 6. (a) RMSD and (b) RMS Fluctuation values for oxadiazole derivative Oxa8 with the transmembrane serine protease 2 (TMPRSS2) PDB ID: 1Z8A

Fig. 6b shows the RMS Fluctuation values for oxadiazole derivative Oxa8 with the transmembrane serine protease 2 (TMPRSS2) PDB ID: 1Z8A. It gives the dynamical behavior of each separate atom present in the ligand as well as backbone of the protein. Including these figures, it may be reported that oxa8 can be the potential candidate to inhibit the viral effect of SARS-CoV-2.

CONCLUSIONS

The coronavirus 2 (SARS-CoV-2) is a highly contagious submicroscopic infectious virus responsible for the COVID-19 pandemic, marked by a devastating loss of lives. Oxadiazole derivatives have garnered attention for their antiviral properties, making them important candidates in the fight against this virus. Examples of such derivatives include CoViTris2020 and ChloViD2020. In an effort to assess their potential, molecular docking and molecular dynamics simulations were conducted for various oxadiazole derivative with key proteins involved in the viral infection process. These proteins include transmembrane serine-2 (TMPRSS2), 3-chymotrypsin-like protease (3CLpro), angiotensin-converting enzyme 2 (ACE2), and papain-like protease (PLpro). The findings of this study revealed that the binding energies of the oxadiazole derivatives were lowest when interacting with TMPRSS2 compared to

the other proteins, namely 3CLpro, ACE2, and PLpro. Specifically, the most stable complex, Oxa8, exhibited a binding energy of -6.52 kcal/mol with TMPRSS2, while the energies with ACE2, 3CLpro, and PLpro were -5.74, -4.55, and -5.56 kcal/mol, respectively. Further analysis through Root Mean Square Deviation (RMSD) during molecular dynamics simulations demonstrated a consistently smooth pattern in the complex structure after 0.6 ns of simulation time. Notably, during the initial 2 ns, the RMSD value for the ligand concerning the protein backbone remained around 2Å, indicating a sustained level of stability. In conclusion, the study suggests that Oxa8 holds promise as a potential candidate for inhibiting the viral activity of SARS-CoV-2, particularly due to its favorable binding interactions with TMPRSS2 and its overall stability in molecular dynamics simulations.

NOTES

The authors declare no competing financial interests.

ACKNOWLEDGMENT

SK thanks Magadh University, Bodh Gaya, Bihar, India for providing lab facility and Science and Engineering Research Board (SERB), Department of Science and Technology (DST), India (Grant No. SRG/2019/002284) for financial support.

REFERENCES

1. Zhou H., Yang J., Zhou C., Chen B., Fang H., *et al*. (2021) Review of SARS-CoV2: compared with SARS-CoV and MERS-CoV. *Front. Med.,* (Lausanne) **8**, 628370. https://doi.org/10.3389/fmed.2021.628370
2. Hoffmann M., Kleine-Weber H., Schroeder S., Kruger N., Herrler T., *et al*. (2020) SARS-CoV-2 cell entry depends on ACE2 and TMPRSS2 and is blocked by a clinically proven proteaseinhibitor. *Cell,* **181**(2), 271-80. https://doi.org/10.1016/j.cell.2020.02.052
3. Cevik M., Tate M., Lloyd O., Maraolo A.E., Schafers J., Ho A. (2021) SARS-CoV-2, SARS-CoV, and MERS-CoV viral load dynamics, duration of viral shedding, and infectiousness: A systematic review and meta-analysis. *Lancet Microbe,* **2**(1), e13-22. https://doi.org/10.1016/S2666-5247(20)30172-5
4. Domling A., Gao L. (2020) Chemistry and biology of SARS-CoV-2. *Chem*., **6**(6), 1283-95. https://doi.org/10.1016/j.chempr.2020.04.023
5. Rabie A.M. (2021) CoViTris2020 and ChloViD2020: A striking new hope in COVID-19 therapy. *Mol. Diversity*, **25**, 1839. https://doi.org/10.1007/s11030-020-10169-0
6. Rabie A.M. (2021) Two antioxidant 2,5-disubstituted-1,3,4-oxadiazoles(CoViTris2020 and ChloViD2020): Successful repurposing against COVID-19 as the first potent multitarget anti-SARS-CoV-2 drugs. *New J. Chem*., **45**, 761. https://doi.org/10.1039/D0NJ03708G
7. Janardhanan J., Chang M., Mobashery S. (2016) The oxadiazole antibacterials. *Current Opinion in Microbiology,* **33**, 13-17. https://doi.org/10.1016/j.mib.2016.05.009
8. Boström J., Hogner A., Llinàs A., Wellner E., Plowright A.T. (2012) Oxadiazoles in medicinal chemistry. *J. Med. Chem*., **55**(5), 1817-30. https://doi.org/10.1021/jm2013248
9. Siwach A., Verma. (2020) Therapeutic potential of oxadiazole or furadiazole containing compounds. *BMC Chemistry,* **14**, 70. https://doi.org/10.1186/s13065-020-00721-2
10. Glomb T., Świątek P. (2021) Antimicrobial activity of 1,3,4-oxadiazole derivatives. *Int. J. Mol. Sci*., **22**(13), 6979. https://doi.org/10.3390/ijms22136979
11. Vaidya A., Jain S., Jain P., Jain P., Tiwari *et al*. (2016) Synthesis and biological activities of oxadiazole derivatives: A review. *Mini Reviews in Medicinal Chemistry,* **16**(10), 825-845. https://doi.org/10.2174/1389557516666160211120835
12. Bajaj S., Roy P.P., Singh J. (2017) 1,3,4-oxadiazoles as telomerase inhibitor: Potential anticancer agents. *Anti-Cancer Agents in Medicinal Chemistry*, **17**(14), 1869-1883. https://doi.org/10.2174/1871521409666170425092906
13. Meng H.W., Shen Z.B., Meng X.S., Yin Z.Q., Wang X.R. *et al*. (2023) Novel flavonoid 1,3,4-oxadiazole derivatives ameliorate MPTP-induced Parkinson's disease via Nrf2/NF-κB signaling pathway. *Bioorg. Chem*., **138**, 106654. https://doi.org/10.1016/j.bioorg.2023.106654
14. Naseem S., Temirak A., Imran A., Jalil S., Fatima S., *et al*. (2023) Therapeutic potential of 1,3,4-oxadiazoles as potential lead compounds for the treatment of Alzheimer's disease. *RSC Adv*., **13,** 17526. https://doi.org/10.1039/D3RA01953E
15. Kumar S. (2022) Curcumin as a potential multiple-target inhibitor against SARS- ip CoV-2 infection: A detailed interaction study using quantum chemical calculations. *J. Serb. Chem. Soc.,* **88**(4), 381-394. https://doi.org/10.2298/JSC220921087K
16. Walls A.C., Park Y.J., Tortorici M.A., Wall A., McGuire A.T., Veesler D. (2020) Structure, function, and antigenicity of the SARS-CoV-2 spike glycoprotein. *Cell,* **181**(2), 281-292. https://doi.org/10.1016/j.cell.2020.02.058
17. Kumar V., Kumar R., Kumar N., Kumar S. (2023) Solvation dynamics of oxadiazoles as potential candidate for drug preparation. *Asian J. Chem.,* **35**. https://doi.org/10.14233/ajchem.2023.27594
18. Somani R.R., Shirodkar P.Y. (2009) Oxadiazole: A biologically important heterocycle *Der Pharma Chemica*,**1**(1), 130-140.
19. Van Der Spoel D., Lindahl E., Hess B., Groenhof G., Mark A.E., Berendsen H.J., (2005) GROMACS: Fast, flexible, and free. *J. Comput. Chem*., **26**,

1701. https://doi.org/10.1002/jcc.20291
20. Bjelkmar P., Larsson P., Cuendet M.A., Hess B., Lindahl E., (2010) Implementation of the CHARMM force field in GROMACS: Analysis of protein stability effects from correction maps, virtual interaction sites, and water models. *J. Chem. Theory Comput*., **6** 459. https://doi.org/10.1021/ct900549r
21. MacKerell A.D.Jr, Banavali N., Foloppe N., (2000) Development and current status of the CHARMM force field for nucleic acids. *Biopolymers*, **56**(4), 257-65. https://doi.org/10.1002/1097-0282(2000)56:4<257::AID-BIP10029>3.0.CO;2-W
22. Kumar S.P., Kumar S., Fazal A.D., Bera S., (2023) Molecular aggregation kinetics of heteropolyene: An experimental, topological and solvation dynamics studies. *Journal of Photochemistry and Photobiology A*: *Chemistry,* **445** 115084. https://doi.org/10.1016/j.jphotochem.2023.115084
23. Kumar S.P., Kumar S., (2023) Weak intra and intermolecular interactions via aliphatic hydrogen bonding in piperidinium based ionic liquids: Experimental, topological and molecular dynamics studies. *J. Mol. Liq.,* **375**, 121354. https://doi.org/10.1016/j.molliq.2023.121354
24. Kumar S., Singh S.K., Vaishnav J.K., Hill J.G., Das A. (2017) Interplay among electrostatic, dispersion, and steric interactions: Spectroscopy and quantum chemical calculations of π-hydrogen bonded complexes. *Chem. Phys. Chem.,* **18**(7), 828-838. https://doi.org/10.1002/cphc.201601405
25. Kumar S., Singh S.K., Calabrese C., Maris A., *et al*. (2014) Structure of saligenin: Microwave, UV and IR spectroscopy studies in a supersonic jet combined with quantum chemistry calculations. *Phys. Chem. Chem. Phys*., **16**, 17163-17171. https://doi.org/10.1039/C4CP01693A
26. Kumar S., Mukherjee A., Das A. (2012) Structure of Indole···Imidazole heterodimer in a supersonic jet: A gas phase study on the interaction between the aromatic side chains of tryptophan and histidine residues in proteins. *J. Phys. Chem.*, A **116**(47), 11573-11580. https://doi.org/10.1021/jp309167a
27. Abraham M.J., Murtola T., Schulz R., Páll S., Smith J.C., *et al.* (2015) GROMACS: High performance molecular simulations through multi-level parallelism from laptops to supercomputers. *SoftwareX,* **1**, 19-25. https://doi.org/10.1016/j.softx.2015.06.001
28. Berendsen H.J., van der Spoel D., van Drunen R. (1995) GROMACS: A message-passing parallel molecular dynamics implementation. *Comput. Phys. Commun*., **91**(1-3)**,** 43-56. https://doi.org/10.1016/0010-4655(95)00042-E